

1 **EXTRACTING URBAN STREET FEATURES USING STREET LEVEL LiDAR DATA**
2 **FOR CONNECTED VEHICLE APPLICATIONS**

3
4
5 **Rakesh Nune, Corresponding Author**

6 District of Columbia Department of Transportation
7 55 M Street, SE, Washington DC 20003
8 Tel: 571-265-4047; Email: Rakesh.Nune@dc.gov

9
10 **Kaiqun Fu**

11 Department of Computer Science
12 Virginia Polytechnic Institute and State University
13 7054 Haycock Rd, Falls Church, VA 22043
14 Tel: 703-303-8419; Email: fukaiqun@vt.edu

15
16 **Jason X. Tao**

17 District of Columbia Department of Transportation
18 55 M Street, SE, Washington DC 20003
19 Tel: 202-671-1489; Email: jason.tao@dc.gov

20
21
22 Word count: 3061 word text + 14 tables/figures x 250 words (each) = 6561
23
24
25
26
27
28
29
30
31
32
33
34
35
36
37
38
39
40
41
42
43

1 **ABSTRACT**

2
3 The connected vehicles and autonomous vehicles have grasped a lot of public attention
4 recently. One of the critical functions for connection vehicle applications is to transmit the
5 roadway MAP data from the Dedicated Short Range Communications (DSRC) roadside
6 equipment to the on-board unit within vehicles. Collection of the MAP data with traditional
7 methodology is very tedious and costly. In this research, we developed an algorithm employing
8 deep learning techniques to extract the lane markings and the stop bar locations from the
9 existing panoramic LiDAR data and images. Previous research work in this direction includes
10 model development based on Bayesian inference road lane detection. As the present work is
11 one of the very first to use street level LiDAR data, a new algorithm is developed based on color
12 clustering and deep learning techniques to identify, classify and geolocate pavement markings.
13 The deep neural network model achieved an accuracy rate of 71.2% in identifying the pavement
14 markings at intersections. The detected pavement markings can be geolocated to generate GIS
15 files which can be used to generate MAP messages. The research work has shown that the
16 proposed approach is promising for the lane detection and road sign recognition thus mapping
17 the city precisely for advancement of connected vehicles.

18
19 **Keywords:** MAP message, DSRC, deep learning, LiDAR, neural network

1 INTRODUCTION

2
3 Connected vehicles have the potential to greatly improve the safety and efficiency of the surface
4 transportation systems. The connected vehicle technology, which includes Vehicle to
5 Infrastructure (V2I) and vice versa communication, provides the functionalities to facilitate
6 autonomous vehicles and driverless operations. In the connected vehicles world, the vehicle
7 On-Board Units (OBU) exchange real-time information with the infrastructure through the DSRC
8 radio for navigation, safety and other operations. In order to get prepared for the coming age of
9 connected vehicle driving, many cities are working towards establishing required infrastructure
10 for enabling smooth transition for connected vehicles (1).

11
12 The content of communication between the vehicles and the infrastructure includes the Signal
13 Phasing and Timing (SPAT), Traveler Information Message (TIM), and the MAP message. The
14 MAP message is a critical component that gives the user information about the geometry of the
15 intersection (2). A typical MAP message contains the data of lane marking, centerline and stop
16 bar locations. Traditionally, the MAP messages are generated manually by using the GIS
17 systems. The methodology requires employing field visits and extensive verifications which is a
18 slow and costly process (3).

19
20 Various early works based on computer vision techniques were proposed for exploring solutions
21 to research challenges of such kinds. For instance, kernel based classification algorithms such
22 as Support Vector Machines (SVM) was raised for road sign recognition (4); other works
23 proposed models based on Bayesian inference were addressed for road lane detection (5).

24
25 The present research work, a methodology using artificial intelligence algorithms like deep
26 learning is proposed to automatically extract pavement marking locations to generate MAP
27 messages for urban areas.

28 29 **Street Level LiDAR Data**

30
31 Light Detection and Ranging (LiDAR) can be categorized into two classes: the airborne LiDAR
32 (ALS) and the terrestrial LiDAR (TLS). The dominant type of LiDAR technology utilized in the
33 studies of urban planning and geomorphology is the topographic LiDAR. The infrared laser light
34 of this type is emitted from a fixed-wing aircraft. The terrestrial LiDAR techniques, on the other
35 hand, usually mounted on moving vehicles, provide much more accurate point collection
36 procedures and can be used to manage facilities, conduct highway and rail surveys.

37
38 Previous studies (6; 7) proposed methods for tropical forest carbon mapping using the airborne
39 LiDAR technologies. Sun et al. (8) proposed an automated method to create 3D watertight
40 building models from airborne LiDAR point clouds. Zhang et al. (9) proposed an optimized
41 segments and connected components classification process, based on the airborne LiDAR
42 data. Although these airborne LiDAR techniques cover a wide ranges of certain regions, they
43 fail to collect dense point clouds with high accuracies as constrained by various limitations (8;
44 9). On the other hand, a few previous works have addressed the feasibility of the terrestrial

45 LiDAR in research purposes. The terrestrial LiDAR techniques can facilitate rapid LiDAR
 46 calibration with minimal field data are developed. Recent years have seen the emergence of the
 47 researches that focus on the terrestrial LiDAR data (10). Research areas such as autonomous
 48 driving, especially in the direction of identification objects obscuring lane marks and road
 49 boundaries, exploited the feasibility of the terrestrial LiDAR data (11). The terrestrial LiDAR data
 50 has been used in resolving the problem of ground roughness estimation for road segmentations
 51 (12). Other works have explored the applicability of the terrestrial LiDAR data in curb and berm
 52 detection (13; 14).

53
 54 In this research, autoencoders, a deep learning algorithm is used to train and recognize the
 55 pavement markings and lane information. Autoencoder is an unsupervised machine learning
 56 algorithm that is capable of extracting hidden features of given high dimension data (15). It is
 57 constructed under the scheme of the feedforward non-recurrent neural networks. It consists of
 58 an input layer, multiple hidden layers and one output layer. The difference between an
 59 autoencoder and a conventional neural network is that size of the output layer in an
 60 autoencoder is the same as the input layer; on the other hand, the output layer of a conventional
 61 neural network is usually smaller than the input layer. Encoders belong to unsupervised
 62 machine learning family unlike conventional neural networks. The two major components: the
 63 encoder and the decoder:

$$\begin{aligned}
 & \phi: \mathcal{X} \rightarrow \mathcal{F} \\
 & \psi: \mathcal{F} \rightarrow \mathcal{X} \\
 & \underset{\phi, \psi}{\operatorname{argmin}} \|X - (\phi \cdot \psi)X\|^2
 \end{aligned} \tag{1}$$

64
 65 where ϕ denotes the encoder, ψ denotes the decoder, and \mathcal{X} , \mathcal{F} denote the input space of the
 66 data and the hidden features space respectively. Equation 1 is the objective function for
 67 minimizing the loss function. Street level Light Detection and Ranging (LiDAR) data is procured
 68 for this work which provides rich data attributes compared to 2D street level imagery.

69
 70 The rest of the paper is organized as follows: the developed algorithm for extracting the street
 71 level data from LiDAR are summarized followed by deep learning technique used to identify the
 72 right pavement marking. The results are discussed in the conclusion section and authors
 73 discussed future work to expand the algorithm to cover other informational signs.

74
 75 **FEATURE DETECTION AND CLASSIFICATION OF STREET LEVEL DATA**

76
 77 The street level LiDAR data is collected by Washington DC department of transportation
 78 collected from a third party provider called Cyclomedia Inc¹. The LiDAR data is overlapped with
 79 street view imagery providing a unique rich data reflecting real world attributes i.e. (X, Y, Z, R,
 80 G, B). Figure 1 shows a typical street level LiDAR image. The algorithm developed in the
 81 project can be divided in to three steps.

¹ Cyclomedia: <http://www.cyclomedia.com/us/>



Figure 1. LiDAR Data at 4th St NW and Decatur St NW

82
83
84
85
86
87
88
89
90
91
92
93

Step 1: Preprocessing of LiDAR cloud and Images

Elevations vary significantly along roadway corridors to accommodate various requirements like drainage, America Disability Act safety requirements. Figure 2 shows heat map of elevation on a typical corridor in Washington DC ranging from lowest elevation shown in blue increasing to red. This presents a challenge in extracting ground LiDAR data that is needed for analysis. To address this issue, corridors are cut regular intervals depending on gradient to generate ground level data

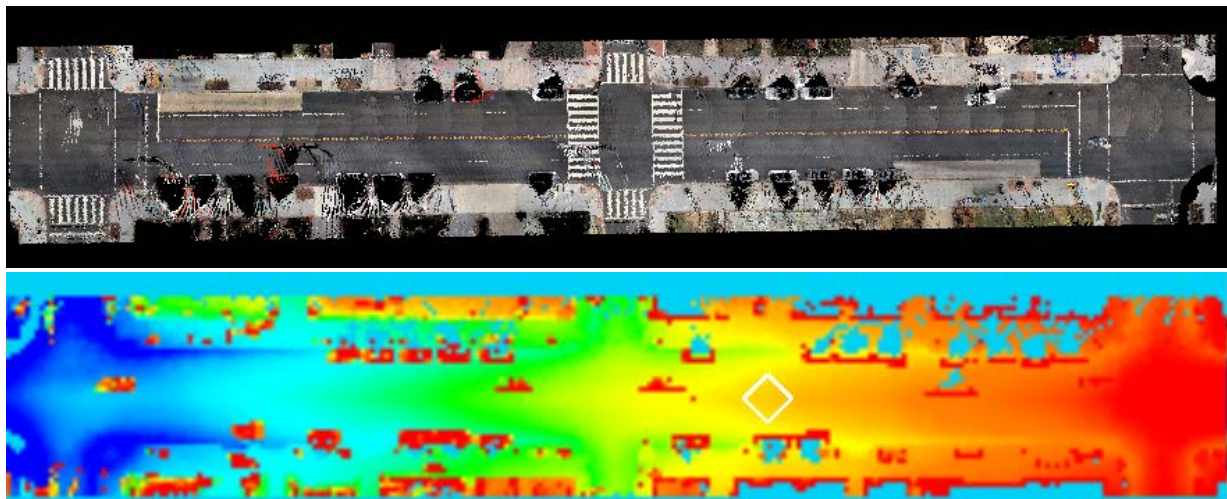


Figure 2: Typical Elevation of Street Profile

94
95
96
97
98
99
100

Depending on the angle of equipment, shadows and presence of other obstacles like vehicles, the quality of LiDAR cloud point data may vary at ground level which is the main interest of our research. Figure 3 shows LiDAR data at an intersection with sparse points on one side.

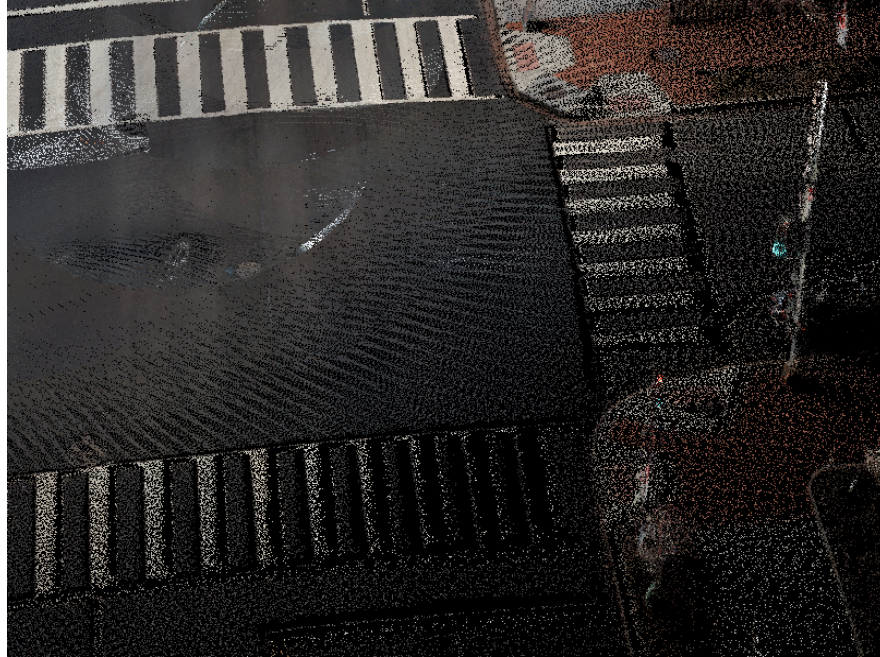


Figure 3. LiDAR picture generated at 16th and R St NW

101
102
103
104
105

Step 2: Clustering the data and image generation

106 In this step, data points are clustered using a distance based clustering method. It was expected
107 that color aggregation would easily separate out pavement markings from background but in
108 reality a huge spectrum of colors was found. Color spectrum occurs because of shadows, bright
109 sunshine and deterioration of infrastructure named *Checker Shadow Illusion*². In order to
110 distinguish the pavement marks from the pavement background, a distance based two-
111 clustering algorithm is used. Due to the extremely large size of the target LiDAR point clouds
112 data set, it is not computationally efficient for the clustering algorithm to consider the entire data
113 set as the input. To increase the efficiency, the Random Sample Consensus (RANSAC)
114 paradigm is utilized with 10% sample rate of the original files. The Random Sample Consensus
115 (RANSAC) algorithm was first proposed to serve as a solution towards the outlier detection
116 problems. It estimates the parameters of a mathematical model from a set of observations
117 which contains outliers in an iterative way. In the proposed coloring clustering task, the intuition
118 of the RANSAC paradigm (16; 17) is referenced, namely, its capability of generalizing large
119 noisy data sets with outliers.

120
121

K-mean clustering algorithm

122 The k-mean clustering algorithm is used on the cloud point with RGB. K-means clustering
123 algorithm partitions the observations of the data points into k clusters, in which each point
124 belongs to the cluster with the closest mean point. In the coloring based clustering scenarios,
125 the data points (pixels) are transformed to the RGB color space, represented by vectors
126 comprise of red, green, and blue channels of the given pixels. More specifically, given a set of

² Checker Shadow Illusion: https://en.wikipedia.org/wiki/Checker_shadow_illusion

127 LiDAR points (pixels) $(\mathbf{p}_1, \mathbf{p}_2, \mathbf{p}_3, \dots, \mathbf{p}_N)$, where each observation of pixel is a 3-dimensional
 128 vector in RGB color space. The k-means clustering algorithm partitions the N observations into
 129 k sets: $\mathcal{S} = \{S_1, S_2, S_3, \dots, S_k\}$ with regard to minimize the sum of squares within clusters:

$$\operatorname{argmin}_S \sum_{i=1}^k \sum_{X \in S_i} \|X - \mu_i\|^2 \quad (2)$$

130 where μ_i is the mean of the points in S_i . In our coloring clustering scenario, under the
 131 assumption that the pixels of the pavement markings differ significantly from the other pixel
 132 points, the parameter k is set to be 2. Note that the target areas are limited to the surface of the
 133 streets in a small range.

134
 135 The mean color calculated in RGB value is represented by a vector with three elements:

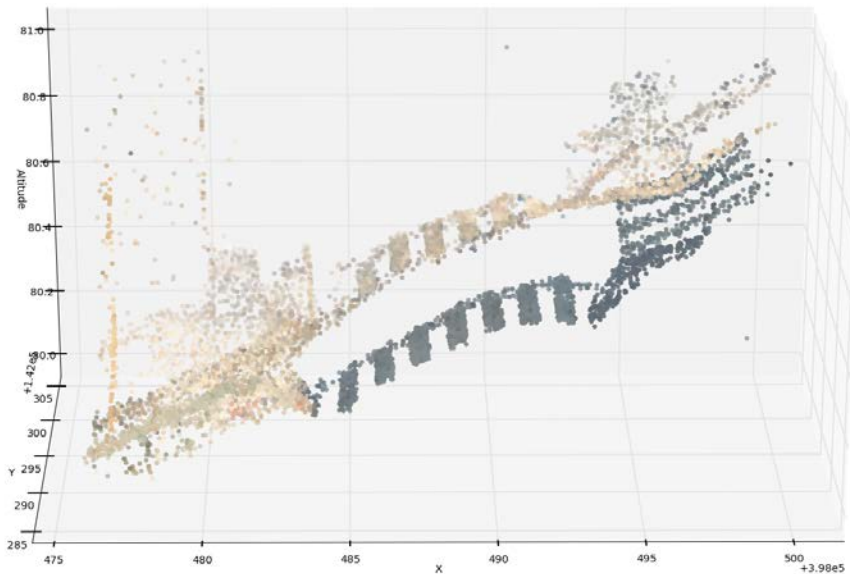
$$\mathbf{C}_{mean} = [R_{mean}, G_{mean}, B_{mean}]^T \quad (3)$$

136 the standard deviation is also represented by a vector of three elements:

$$\mathbf{C}_{std} = [R_{std}, G_{std}, B_{std}]^T \quad (4)$$

137 According to the calculated means and standard deviations, the filtering process filters the point
 138 cloud by applying the following threshold with a 3-std:

$$\mathbf{C}_{range}: [\mathbf{C}_{mean} - 3\mathbf{C}_{std}, \mathbf{C}_{mean} + 3\mathbf{C}_{std}] \quad (5)$$



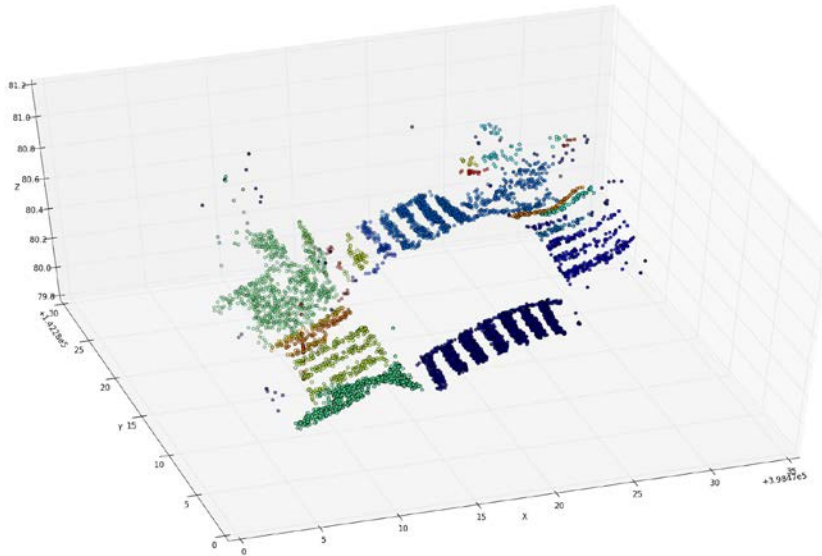
139
 140

Figure 4. Clustering based on pixel colors

141 Upon clustering the points, DBSCAN (18), a density based spatial clustering algorithm, is
142 performed on selected points to pinpoint the location and visualize the boundaries of the
143 pavement marks.

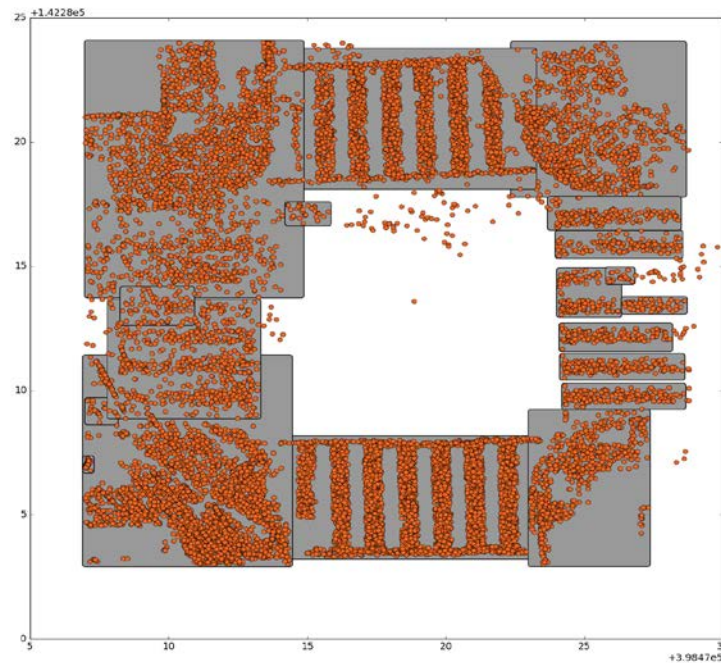
144
145 Figure 5(a) shows clustering of LiDAR data based on coloring scheme. Figure 5(b) shows the
146 clusters in two dimensions. The clusters then converted to images as shown in Figure 6. These
147 images will be used as input for deep learning algorithms in step 3 to identify pavement marking
148 from noise like curbs, cars and other infrastructure.

149



150
151

Figure 5(a). Spatial Clustering of LiDAR Data point data



152
153

Figure 5(b). 2D clustering of data generated from 5(a)

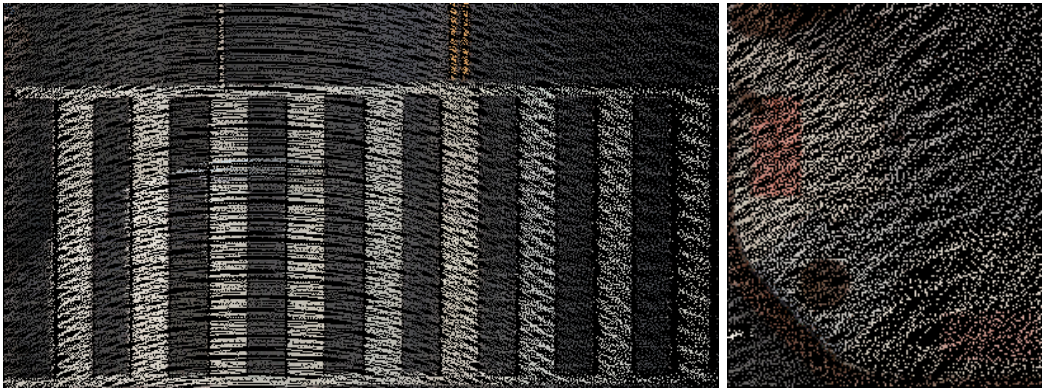


Figure 6. Images generated from spatially clustered images

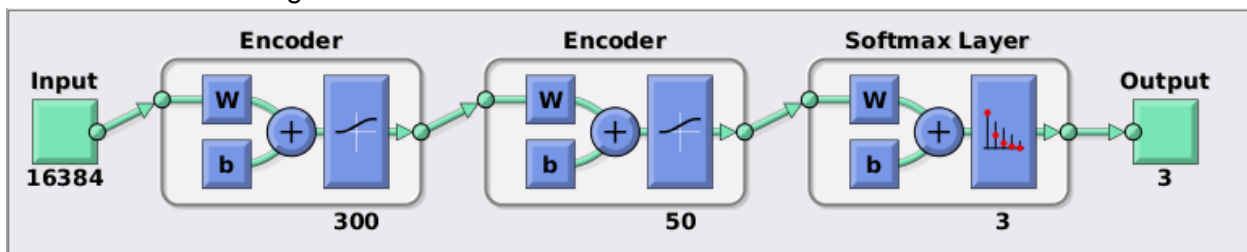
155
156
157
158
159

Step 3: Classification and Plotting of generated data using Deep Learning Techniques

160 The present work implemented autoencoder from deep learning techniques. Autoencoder is
161 known for its promising performance in extracting and identifying features in high dimensional
162 spatial data. The terrestrial LiDAR data is extremely dense and also has six dimensions which
163 results in computationally intensive neural network model so for this work the dimension have
164 been reduced to three i.e. just position data for training the model. The training data contains
165 128 road sections in Washington D. C., with an overall size of 18.1 GB. The 16th street NW
166 corridor between T St NW and Church St NW is selected for testing the developed model. A
167 total of 900 top view images of various intersections in Washington DC were used for training
168 the autoencoder mode. Four intersections are selected for testing data generation consisting a
169 total of 132 labelled data.

170

171 The algorithm is implemented on Ubuntu 14.04 system with a Python version 2.7, MATLAB
172 2015b³. The LibLAS⁴ library is used for LiDAR data preprocessing and analysis. Python module
173 PyProj⁵ is utilized for cartographic transformations and geodetic computations. The autoencoder
174 is constructed by using Neural Networks Toolbox provided by MATLAB 2015b. The layer of the
175 autoencoder consists of 16384 feature nodes from the pavement markings proposal images.
176 Two layers of encoder are implemented, the detailed configurations for each layers are listed
177 below and shown in figure 7.



178
179

Figure 7: Neural Network Model Developed for Classification

³ MATLAB: http://www.mathworks.com/products/new_products/latest_features.html

⁴ LibLAS: <http://www.liblas.org/>

⁵ PyProj: <https://jswhit.github.io/pyproj/>

180 **RESULT DISCUSSION**

181

182 The above autoencoder model has achieved an accuracy of 71.2% in classifying the data to
183 right category which is plotted on map and shown in Figure 8(a). The green bounding boxes
184 represent the pavement markings predicted by algorithm and Red boxes show noise recognized
185 by the model between 16 St NW between N St and T St NW. Figure 8(b)-8(d) shows individual
186 intersections.

187



188

189

190

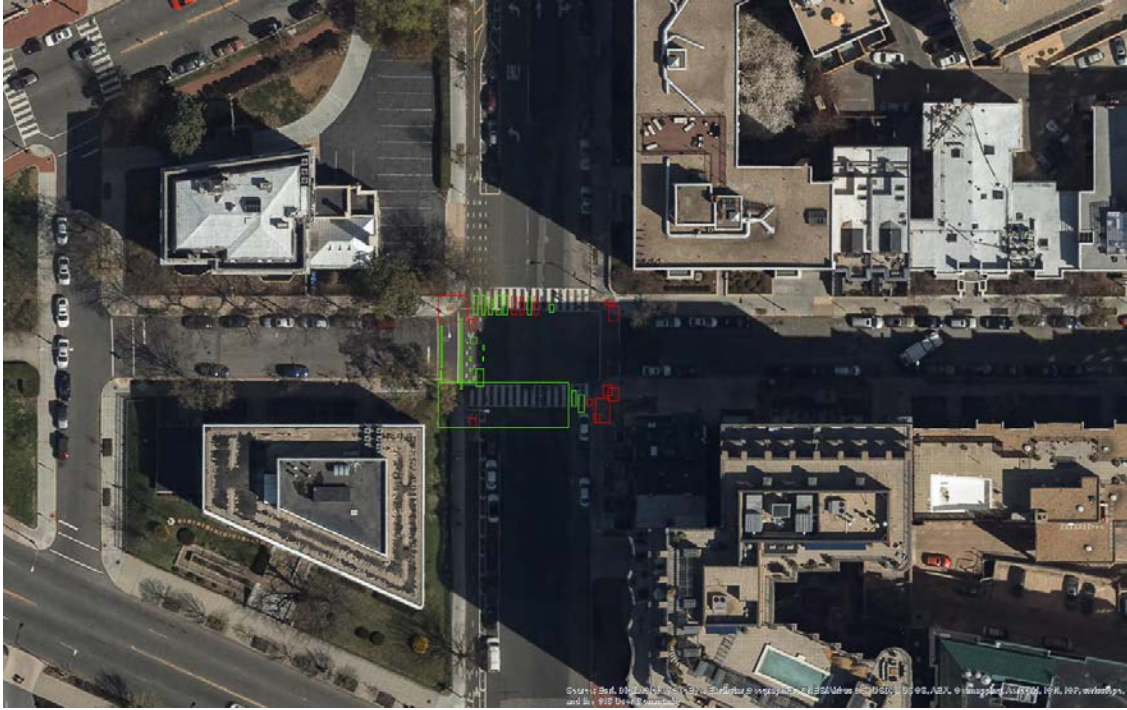
Figure 8(a): Detected pavement marking on 16th St



191

192

Figure 8(b): Detected pavement marking on 16th St and Church St NW



193
194
195

Figure 8(c): Detected pavement marking on 15th and N St NW



196
197
198

Figure 8(d): Detected pavement marking on 16th and Corcoran St NW

199 Accuracy rates can be further improved by training the model with more data and especially with
 200 better quality. For example Figure 9 shows an intersection at Church St with low data density
 201 which is reflected in the model prediction inaccuracy in Figure 8(b). Table 1 shows the total area
 202 to be recognized, area with bad data and actual recognized pavement markings by developed
 203 algorithm. It can be seen that good data is available only for approximately 77%.



Figure 9: Intersection level LiDAR data at 16th and Church St NW

Table 1: Intersection level LiDAR Data Statistics

| Total Area Pavement markings area (Sq Ft) | Bad LiDAR data Area (Sq Ft) | Detected Area (Sq Ft) |
|---|-----------------------------|-----------------------|
| 9453 | 2178 | 5246 |

CONCLUSION AND FUTURE WORK

The research is pioneering work in using street level LiDAR data, as we continue working on algorithms and procure more data, accuracy will improve. Future work will concentrate on developing algorithms to generate missing LiDAR data which will improve accuracy. Immediate further work will focus on detecting road signs, road symbols and also reading the data. The generated data will be then converted into the MAP message and will be available for public usage to be implemented in connected vehicle demonstrations.

ACKNOWLEDGMENTS

The authors would like to acknowledge the support received from District Department of Transportation (DDOT) for implementing the project especially from IT department for providing the data.

REFERENCES

- [1] Vock, D. C. In Preparation for Driverless Cars, States Start Upgrading Roads. In *Governing*, governing.com, 2016.
- [2] Kenney, J. B. Dedicated short-range communications (DSRC) standards in the United States. *Proceedings of the IEEE*, Vol. 99, No. 7, 2011, pp. 1162-1182.
- [3] Xu, Q., T. Mak, J. Ko, and R. Sengupta. Vehicle-to-vehicle safety messaging in DSRC. In *Proceedings of the 1st ACM international workshop on Vehicular ad hoc networks*, ACM, 2004. pp. 19-28.
- [4] Bascón, S. M., J. A. Rodríguez, S. L. Arroyo, A. F. Caballero, and F. López-Ferreras. An optimization on pictogram identification for the road-sign recognition task using SVMs. *Computer Vision and Image Understanding*, Vol. 114, No. 3, 2010, pp. 373-383.

233 [5] Nieto, M., J. A. Laborda, and L. Salgado. Road environment modeling using robust
234 perspective analysis and recursive Bayesian segmentation. *Machine Vision and Applications*,
235 Vol. 22, No. 6, 2011, pp. 927-945.

236 [6] Asner, G. P., J. Mascaro, H. C. Muller-Landau, G. Vieilledent, R. Vaudry, M. Rasamoelina, J.
237 S. Hall, and M. van Breugel. A universal airborne LiDAR approach for tropical forest carbon
238 mapping. *Oecologia*, Vol. 168, No. 4, 2012, pp. 1147-1160.

239 [7] Mascaro, J., M. Detto, G. P. Asner, and H. C. Muller-Landau. Evaluating uncertainty in
240 mapping forest carbon with airborne LiDAR. *Remote Sensing of Environment*, Vol. 115, No. 12,
241 2011, pp. 3770-3774.

242 [8] Sun, S., and C. Salvaggio. Aerial 3D building detection and modeling from airborne LiDAR
243 point clouds. *IEEE Journal of Selected Topics in Applied Earth Observations and Remote*
244 *Sensing*, Vol. 6, No. 3, 2013, pp. 1440-1449.

245 [9] Zhang, J., X. Lin, and X. Ning. SVM-based classification of segmented airborne LiDAR point
246 clouds in urban areas. *Remote Sensing*, Vol. 5, No. 8, 2013, pp. 3749-3775.

247 [10] Huang, A. S., D. Moore, M. Antone, E. Olson, and S. Teller. Finding multiple lanes in urban
248 road networks with vision and lidar. *Autonomous Robots*, Vol. 26, No. 2-3, 2009, pp. 103-122.

249 [11] Hernández, J., and B. Marcotegui. Filtering of artifacts and pavement segmentation from
250 mobile lidar data. In *ISPRS Workshop Laserscanning 2009*, 2009.

251 [12] Urmson, C., J. Anhalt, D. Bagnell, C. Baker, R. Bittner, M. Clark, J. Dolan, D. Duggins, T.
252 Galatali, and C. Geyer. Autonomous driving in urban environments: Boss and the urban
253 challenge. *Journal of Field Robotics*, Vol. 25, No. 8, 2008, pp. 425-466.

254 [13] Kammel, S., and B. Pitzer. Lidar-based lane marker detection and mapping. In *Intelligent*
255 *Vehicles Symposium, 2008 IEEE*, IEEE, 2008. pp. 1137-1142.

256 [14] Cremean, L. B., and R. M. Murray. Model-based estimation of off-highway road geometry
257 using single-axis lidar and inertial sensing. In *Proceedings 2006 IEEE International Conference*
258 *on Robotics and Automation, 2006. ICRA 2006.*, IEEE, 2006. pp. 1661-1666.

259 [15] Vincent, P., H. Larochelle, I. Lajoie, Y. Bengio, and P.-A. Manzagol. Stacked denoising
260 autoencoders: Learning useful representations in a deep network with a local denoising
261 criterion. *Journal of Machine Learning Research*, Vol. 11, No. Dec, 2010, pp. 3371-3408.

262 [16] Fischler, M. A., and R. C. Bolles. Random sample consensus: a paradigm for model fitting
263 with applications to image analysis and automated cartography. *Communications of the ACM*,
264 Vol. 24, No. 6, 1981, pp. 381-395.

265 [17] Fontanelli, D., L. Ricciato, and S. Soatto. A fast ransac-based registration algorithm for
266 accurate localization in unknown environments using lidar measurements. In *2007 IEEE*
267 *International Conference on Automation Science and Engineering*, IEEE, 2007. pp. 597-602.

268 [18] Ester, M., H.-P. Kriegel, J. Sander, and X. Xu. A density-based algorithm for discovering
269 clusters in large spatial databases with noise. In *Kdd*, No. 96, 1996. pp. 226-231.

270